Special Issue

New Insights Into the Development and Progression of Geographic Atrophy After Full Thickness Autologous Choroidal Graft

Grazia Pertile,[1] Maurizio Mete,[1] Antonio Peroglio Deiro,[1,2] Massimo Guerriero,[3] Mauro Sartore,[1] Alessandro Alfano,[1] and Antonio Polito[1]

[1]Department of Ophthalmology, Sacro Cuore Don Calabria Hospital, Negrar, Verona, Italy
[2]Department of Ophthalmology, San Gerardo Hospital, Monza, Milan, Italy
[3]Department of Computer Science, University of Verona, Verona, Italy

Correspondence: Grazia Pertile, Sacro Cuore Don Calabria Hospital, Via don Sempreboni, 5 Unità Operativa di Oculistica, Negrar 37024, Verona, Italy;
grazia.pertile@sacrocuore.it.

Submitted: March 1, 2018
Accepted: June 5, 2018

Citation: Pertile G, Mete M, Peroglio Deiro A, et al. New insights into the development and progression of geographic atrophy after full thickness autologous choroidal graft. *Invest Ophthalmol Vis Sci*. 2018;59:AMD93–AMD103. https://doi.org/10.1167/iovs.18-24229

Purpose. To investigate if the contiguity between native and transplanted retinal pigment epithelium (RPE) represents a protective factor against the progression of atrophy after autologous choroidal graft. In addition, the changes in fundus autofluorescence (FAF) in the contiguous and noncontiguous RPE areas were explored.

Methods. The first postoperative reliable FAF image was selected and divided into sectors based on the characteristics of the RPE at the edge of the graft. The sectors were categorized into three groups: contiguous RPE, noncontiguous RPE, and not classifiable. The area of RPE atrophy, inside and outside the graft, was measured for each sector at baseline, one, three, and five years of follow-up. The FAF pattern outside the graft was evaluated for every sector at baseline and during the follow-up.

Results. Nineteen patients met the inclusion criteria and were included in this study. Trend analysis showed that the atrophy progression outside the graft was statistically significant in areas where native and transplanted RPE were noncontiguous ($P < 0.0001$) yet not so in contiguous areas ($P < 0.058$). Inside the graft, both groups showed an increase in atrophy over time. In addition, the noncontiguous group developed more severe increased FAF patterns compared with the contiguous group.

Conclusions. RPE contiguity after autologous choroidal graft seems to be a protective factor against atrophy progression, whereas any area of damaged or absent RPE tends to enlarge over time. This may suggest that the transplantation of an RPE sheet is more likely to be effective than an RPE cell suspension.

Keywords: choridal graft, geographic atrophy, age-related macular degeneration, choridal transplantation

In developed countries, age-related macular degeneration (AMD) is the leading cause of legal blindness in the elderly.[1] The introduction of antivascular endothelial growth factor (anti-VEGF) therapy for exudative AMD represents a milestone in the treatment of this disease.[2] Nevertheless, there is evidence of the frequent progression of atrophic degeneration, despite good control of the neovascular component of the disease.[3–5]

During the past decade, a major effort has been made to understand the pathophysiology of AMD. This represents the first step toward new therapeutic frontiers. As there is a symbiotic relationship between photoreceptors, retinal pigment epithelium (RPE), Bruch's membrane, and choriocapillaris (CC), an alteration in a single component of the complex can initiate a cascade of events that compromise the whole system.[6] Consequently, it can be difficult to identify the initial cause. The two types of AMD, atrophic and exudative, may have different etiologies. McLeod et al.[7] observed a loss of CC with a normal RPE monolayer in wet AMD, whereas the RPE was affected first in geographic atrophy (GA).

Therefore, it can be particularly interesting to study what happens to a healthy CC-RPE complex when it is positioned under the macula of an eye affected by AMD. Apart from experimental RPE transplantation, this can be achieved using one of two surgical techniques: macular translocation, which involves rotation of the macula over a healthy area of RPE and choroid, or autologous choroidal transplantation, in which a full thickness choroidal graft is positioned under the macula after the removal of choroidal neovascularization (CNV).

Many authors have described a significantly enlarged atrophic area correlated with CNV removal.[8–11] Moreover, the appearance of recurrent RPE atrophy underneath the new position of the macula was reported after full macular translocation for dry AMD.[12–14] This may suggest that the diseased retina retains a pathogenic stimulus that can influence the underlying healthy RPE.

In addition, we observed that areas of severe atrophy progression can coexist with areas of perfect RPE preservation in the same eye after autologous choroidal transplantation. We further noticed that areas in which native RPE was contiguous with transplanted RPE were less likely to develop atrophic changes compared with noncontiguous areas between native and transplanted RPE.

The aim of this study is to investigate if there is differing behavior between areas in which native RPE is adjacent to transplanted RPE and areas in which there is noncontiguity between the two layers, with respect to atrophy progression and fundus autofluorescence (FAF) pattern.

Methods

This is a single-center, observational, retrospective study of consecutive, uncontrolled cases. It was approved by the institutional review board. The study was carried out in accordance with the Declaration of Helsinki.

Patient Cohort

The charts of patients who underwent RPE-choroid graft transplantation in the Sacro Cuore Don Calabria Hospital, Italy, from 2007 to 2013 were reviewed. This surgery was offered to patients with (1) decreasing visual acuity caused by active CNV despite repeated anti-VEGF injections (nonresponder), (2) an RPE tear involving the fovea, (3) subfoveal fibrosis and visual loss with preservation of the external limiting membrane on spectral-domain optical coherence tomography (SD-OCT), or (4) a large submacular hemorrhage that could not be sufficiently displaced with tissue plasminogen activator injection.

Informed patient consent was obtained after the patients had been made fully aware of the benefits and risks of the surgery. Best-corrected visual acuity (BCVA), fundus examination, SD-OCT, and FAF (Heidelberg Engineering, Heidelberg, Germany) were assessed before surgery and at every follow-up visit. Imaging with FAF, fluorescein angiography (FAG), indocyanine green angiography (ICGA), and SD-OCT (Spectralis Heidelberg retinal angiography + OCT [HRA-OCT]; Heidelberg Engineering) were obtained preoperatively in all the patients with clear optical media and during the follow-up at physician discretion. The anatomic and functional results of the whole cohort of patients who underwent this surgery at Sacro Cuore Hospital from 2007 to 2013 have already been reported.[15] For this study, only patients with follow-up longer than five years and with SD-OCT and FAF images obtained regularly during the follow-up were included.

Surgical Procedures

Previous research has described the surgical techniques used in this study.[15,16] In summary, after a complete vitrectomy, the temporal retina was detached using a 41-gauge needle for a subretinal balanced salt solution injection. Next, a peripheral retinotomy was performed. The CNV was then removed and the feeder choroidal vessel coagulated. Afterward, a suitable harvesting area was identified and a free graft was prepared and positioned under the macula. Special attention was paid in the selection of the harvesting zone. Big choroidal vessels needed to be avoided to reduce the risk of postoperative subretinal hemorrhages. Moreover, it is important to harvest the graft outside the posterior pole, because this seems to increase the risk of the formation of a fibrotic ring around the choroidal patch. At the same time, taking the graft close to the ora serrata might interfere with the laser treatment of the edge of the retinotomy and, therefore, influence the incidence of proliferative vitreoretinopathy. These limitations can impact the size of the graft. Finally, the retina was reattached and silicone oil was used as a tamponade. The silicone oil was removed after one to four months.

Imaging Procedures

Spectral-Domain Optical Coherence Tomography. The Spectralis HRA-OCT protocol was comprised of a standard of 49 B-scans per volume scan, with a width and height of 20×20 degrees. Each scan was averaged using the automated real-time mode of the Spectralis device, with 30 frames per B-scan. The follow-up function of the Spectralis system was used throughout the study to ensure that the B-scans were performed in the same position in all examinations.

Fundus Autofluorescence. For FAF, the confocal scanning laser ophthalmoscopy device of the Spectralis HRA-OCT uses a wavelength of 488 nm. The FAF images were acquired with a frame size of 30×30 degrees and a resolution of 768×768 pixels. The software provides an "automatic real-time" (ART) function to reduce noise and increase image quality. With ART activated, multiple images of the same scanning location were performed during the scanning process, and only images with elevated ART (range, 50–99) were considered.

Outcome Measures

Demographics, clinical data, and images were reviewed from all patient files. Cohort patients were assessed one month postoperatively with FAG and ICGA to ascertain if reperfusion of the choroidal graft had taken place.

The evaluation chosen as baseline coincided with the first postoperative reliable FAF within three months after the surgery, regardless of the presence of silicon oil. Further assessments were made at one, three, and five years of follow-up. At each time point, a complete ophthalmic evaluation, SD-OCT, and FAF were performed.

Study Design

Given the lack of a standardized method for comparing postgraft atrophy progression over time, the study design required innovation. To achieve this, an overlay was created and placed over FAF images from baseline to the 5-year follow-up, thus enabling a precise visual guide to assess the area of atrophy in corresponding sectors at different time points (Fig. 1).

As such, a patch contour was first outlined at the baseline FAF by using the Heidelberg Eye Explorer software (version 1.9.13.0) "draw region" tool. This provided the base of the overlay (Fig. 1A). To maximize the reliability of the graft profiles, SD-OCT and FAF were simultaneously evaluated. Second, the center of the fovea was identified by comparing FAF and SD-OCT. Third, the areas in which the graft's RPE was contiguous with the native RPE (hereafter referred to as "contiguous areas") were identified and delineated from areas in which the edge of the graft was in contact with a zone denuded from the RPE during the CNV removal maneuver (hereafter referred to as "noncontiguous areas"). This third step was performed by drawing lines starting from the fovea and intersecting the point of transition between contiguous and noncontiguous RPE areas (Fig. 1B).

Fourth, areas in which it was not possible to clearly define the RPE condition at the edge of the graft were not considered for the atrophy progression analysis and were marked as NC (nonclassifiable). This was usually correlated with the presence of some blood at the margin of the patch. Another reason for excluding a sector was the development of a CNV at the perimeter of the transplant. This latter condition occurred in certain cases during the follow-up but remained confined to the border of the graft and did not usually require treatment. The arrow in Figure 1C indicates the hyperreflective material at the edge of the graft that corresponds to the neovascular tissue. The extension of the CNV was assessed on FAG. The

Investigative Ophthalmology & Visual Science

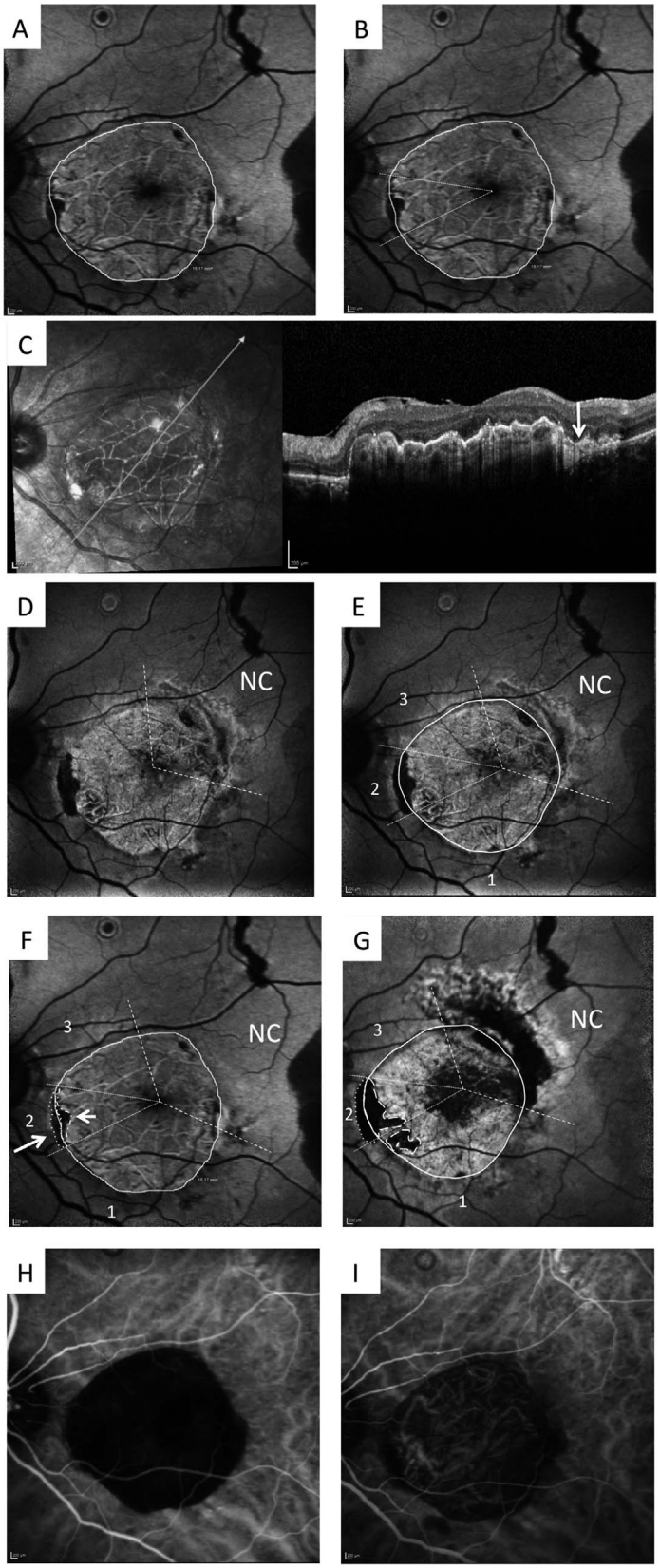

FIGURE 1. Method used for the evaluation of GA progression after choroidal transplantation. The patch contour was outlined on the first reliable postoperative FAF (**A**). The center of the fovea was identified, and lines were drawn starting from the fovea center and intersecting the point of transition between contiguous and noncontiguous RPE areas (**B**). The extension of areas that developed a neovascular membrane at the edge of the graft, at any time point, were evaluated on FAG and SD-OCT (**C**) and then marked as NC and demarcated with a *dotted line* (**D**). The remaining sectors were numbered clockwise (**E**). The entire overlay was then copied and pasted over the FAF image from baseline (**F**), 1-, 3-, and 5-years follow-up (**G**). The atrophy in each sector at every time point was measured. In addition, ICGA was used to assess graft reperfusion. A graft with a dark appearance without any choroidal vessel detectable was considered as a nonperfused transplant (**H**), whereas the presence of a choroidal network independent from the underlying choroidal vasculature proved its reperfusion (**I**).

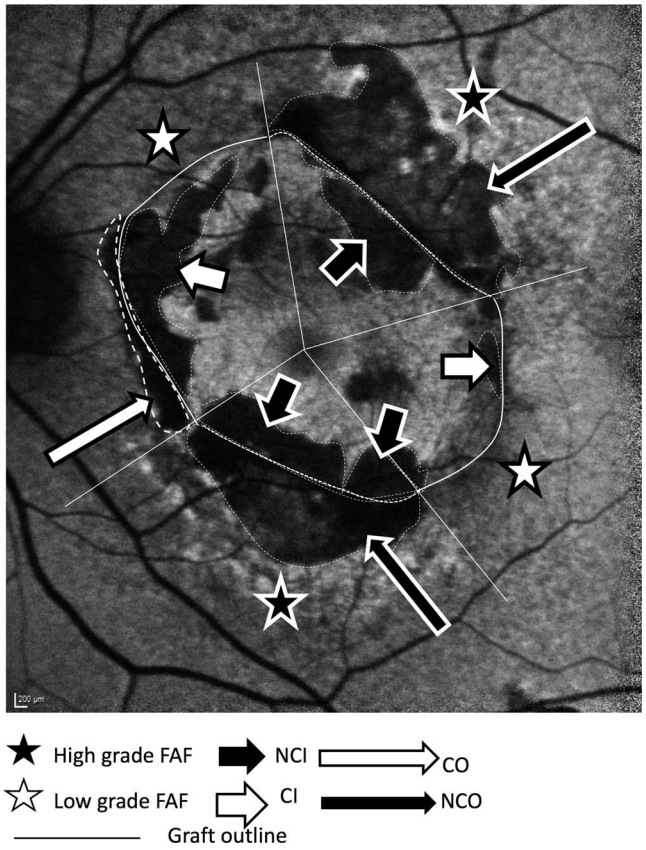

FIGURE 2. The four categories of atrophy were represented in this figure: contiguous inside (CI) (*short white arrow*), contiguous outside (CO) (*long white arrow*), noncontiguous inside (NCI) (*short black arrow*), noncontiguous outside (NCO) (*long black arrow*) as well as two sectors of high-grade FAF pattern (*black stars*) and two sectors of low-grade FAF pattern (*white stars*).

corresponding sector was labeled as NC (Fig. 1D) and was examined separately. Fifth, and finally, the remaining sectors were numbered clockwise to permit the atrophy progression assessment in the same sector at different time points (Fig. 1E). This completed the overlay creation process.

With the overlay complete, measuring atrophy areas in different sectors could begin. To do so, the entire overlay was copied and pasted over FAF images at baseline, one-, three-, and five-year follow-up for each patient (Region Finder Module, version 2.6.2.0; Heidelberg Engineering). At least five reference points were used to ensure consistency and accuracy in pasting the overlay on each FAF image (Supplementary Fig. S1). The areas of RPE atrophy inside the graft (Fig. 1F, short arrow) and outside it (Fig. 1F, long arrow) were measured at the baseline FAF for each sector. The same procedure was then repeated for each image at the different time points (Fig. 1G).

As a result of this operation, we were able to divide the atrophy areas into four groups: atrophy in a contiguous area inside the graft (CI), contiguous outside the graft (CO), noncontiguous areas inside the graft (NCI), and noncontiguous areas outside the graft (NCO), as represented in detail in Figure 2. The sum of the RPE atrophy areas for every group was calculated at each time point. In most of the cases, the atrophy areas inside the transplant at baseline were correlated with iatrogenic damage caused by the forceps during their positioning.

The areas of RPE atrophy tended to enlarge centrifugally as well as laterally. As a consequence, there may have been a diffusion of the atrophy from one sector to another, which made the measurement somewhat approximate. One case presented in Figure 3 (I–L) shows an example of this phenomenon; the white arrow on the upper-left (Fig. 3J, baseline FAF) shows a thin area of contiguous RPE that was subsequently replaced by atrophy, which was most likely influenced by the adjacent NCO areas (starred in Figs. 3K, 3L).

In addition, the FAF pattern was recorded for each sector outside the patch by using the classification proposed by Schmitz-Valckenberg et al.,[17] which described four different patterns: absent, focal, banded, and diffuse. To simplify the analysis, we considered two stages, being a low FAF pattern (absent or focal) and a high FAF pattern (banded or diffuse), as represented in Figure 2 (white and black stars). The FAF pattern in the sectors inside the choroidal graft could not be evaluated because of an uneven graft surface. The scan evaluation was performed by two experienced observers (MM and APD).

Statistical Analysis

Results are expressed as mean and standard deviation if variables are continuous and as a percentage if variables are categoric. The Shapiro-Wilks test was used to test normality for continuous variables.

The paired *t*-test or Wilcoxon matched-pairs signed-ranks test was used to compare the mean of continuous variables at baseline versus the mean at the different follow-ups. To analyze the atrophy progression trend in the CO, NCO, CI, and NCI areas, a trend test with corrections for ties was used. Trend analysis is, fundamentally, a method for understanding how and why things have changed or will change over time. It is a statistical approach to analysis that collates data and then attempts to discover patterns, or trends, within that data for the purposes of understanding or predicting behaviors. The interrater agreement with two unique raters was evaluated with Cohen's K statistic. A P value < 0.05 was considered statistically significant. Analyses were performed using STATA version 15 (StataCorp, College Station, TX, USA).

RESULTS

A total of 27 patients reached at least 5-years follow-up, but only 19 that had gradable FAF and OCT images throughout the follow-up period could be enrolled. The most frequent cause for exclusion was the presence of an area of atrophy that fell outside the standard 30-degree FAF image, making the atrophy progression assessment impossible.

The Table reports the patients' demographics (age, BCVA at different time points, timing of graft reperfusion, and the total atrophy area in the four sectors). The mean age of the patients at the time of surgery was 76.04 (SD 9.52) years and 55% were female. Six patients lost two or more lines of BCVA during the follow-up compared with the BCVA achieved after surgery. Three eyes developed RPE and outer retina atrophy during the follow-up, whereas three other eyes needed treatment for recurrent subfoveal CNV. The mean area of the graft was 16.71 (SD 5.75) mm^2. The mean baseline atrophic area was 6.78 (SD 1.87) mm^2 in the NCO areas and 0.83 (SD 0.62) mm^2 in the CO zones. The difference was statistically significant ($P < 0.0001$). Figure 4 shows the mean change in atrophic area outside the graft at the different time points. Trend analysis revealed that the atrophy progression was statistically significant among the NCO areas ($P < 0.0001$) but not so in the CO areas ($P < 0.058$). In fact, even the CO areas demonstrated a slight increase in atrophy during the follow-up. This phenomenon is

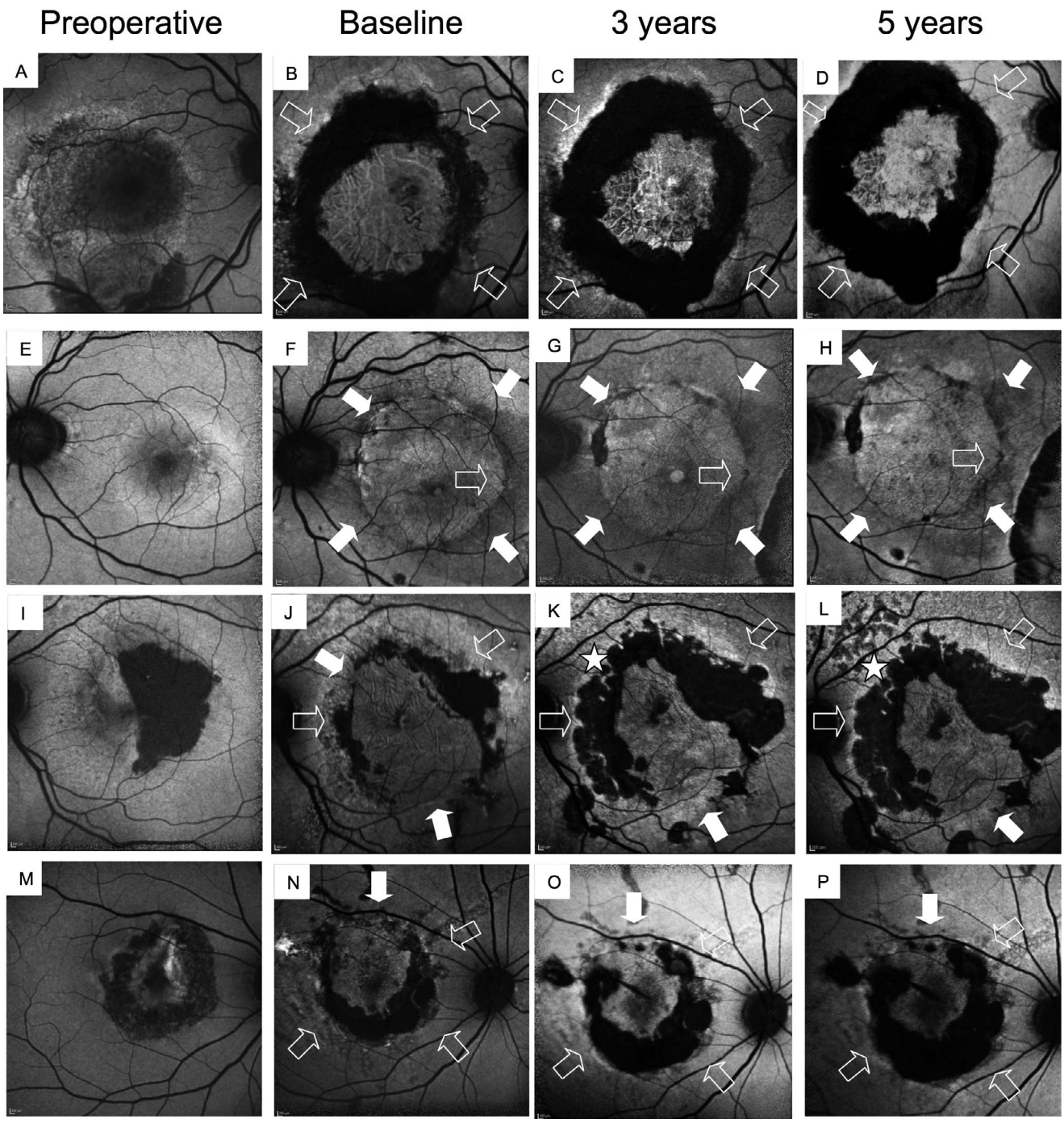

FIGURE 3. Representative examples of atrophy progression in four patients during follow-up. The *full arrows* indicate the areas where the native and transplanted RPE are contiguous, whereas the *empty arrows* indicate where RPE are not noncontiguous. In the first case (**A–D**), the graft has no point of contiguity with the native RPE. During the follow-up, there is a significant progression of GA that involves both the native and transplanted RPE. In the second case (**E–H**), the graft almost completely covers the RPE defect originating from CNV removal. There is only a small RPE defect (*short empty arrow*) that enlarges slightly over time. After five years, the remaining RPE shows an overall normal FAF and no sign of GA. In the last two cases (**I–L**, **M–P**) contiguous RPE areas outside the graft (CO) coexist with noncontiguous areas (NCO). The NCO areas show a remarkable progression of GA, whereas in the CO areas, the FAF is preserved, except for narrow contiguous areas (**J**, *full arrow upper left*), which are likely to be invaded from the adjacent developing atrophy (**K**, **L**, *starred*).

likely to be influenced by the lateral progression of atrophy from the NCO areas, which tends to invade the CO sector (starred in Figs. 3K–L).

At baseline, the atrophic surface inside the graft is quite limited in both groups: 0.45 (SD 0.13) mm^2 and 0.11 (SD 0.04) mm^2, respectively, for the NCI and CI areas ($P < 0.0001$). This is mainly due to the iatrogenic damage to the choroidal patch where it was grasped for proper positioning during the surgery. The trend analysis shows a statistically significant increase in atrophy over time in both groups. Nevertheless, the NCI group exhibits a more rapid progression compared with the CI group (Fig. 5).

Table. Patient Demographics

		BCVA (dec.)				Graft Perfusion		Atrophy at Baseline, mm^2				Atrophy at 1 Year FU, mm^2				Atrophy at 3 Years FU, mm^2				Atrophy at 5 Years FU, mm^2			
Id	Age, y	Preop	1 y	3 y	5 y	Within 1 Month	Overall	CI	CO	NCI	NCO	CI	CO	NCI	NCO	CI	CO	NCI	NCO	CI	CO	NCI	NCO
1	60	0.15	0.4	0.5	0.5	Yes	Yes	0.62	0.5	0	1	1.12	1.09	0	1.21	1.41	1.19	0	1.39	2.27	1.41	1.13	1.51
2	80	HM	0.1	0.1	0.1	Yes	Yes	0	0.58	0.61	17.63	0	0.65	0.67	20.06	0.08	0.71	0.71	28.21	0.06	0.34	0.63	34.02
3	77	0.05	0.2	0.2	0.3	Yes	Yes	0.2	0.71	0	10.38	0.2	0.93	0.1	12.24	0.24	1.04	0.25	13.68	0.26	1.63	1.01	13.65
4	80	0.3	0.6	0.5	0.4	Yes	Yes	0	0.87	N/A	N/A	18.75	1.99	N/A	N/A	19.75	4.86	N/A	N/A	22.15	5.4	N/A	N/A
5	85	0.1	0.4	0.6	0.1	Yes	Yes	0.43	0	0.62	18.09	0.35	0.46	3.76	18.66	0.56	2.45	3.85	25.29	0.79	12.25	3.83	17.82
6	70	0.25	0.2	0.25	0.2	Yes	Yes	0	0	0.22	0.79	0	0	0.75	0.8	0.75	0.18	1.12	1.87	0.84	0.18	1.25	2.01
7	81	0.4	0.5	0.5	0.4	Yes	Yes	0	0	0.8	13.71	0.29	0.09	2.96	14.14	0.08	0.14	2.88	14.07	0.22	0.36	5.57	17.58
8	74	0.1	0.4	0.3	0.2	Yes	Yes	0	15.63	0.66	0.48	0	19.55	1.14	0	0.29	15.41	1.02	0.24	1.18	16.52	1.32	0
9	65	HM	0.1	0.3	0.3	No	Yes	N/A	N/A	2.9	33.11	N/A	N/A	7.25	42.9	N/A	N/A	11.26	43.68	N/A	N/A	12.36	44.18
10	63	0.3	0.2	0.1	CF	No	Yes	0.11	0	0.44	0	0.2	0.45	0.32	0.46	0.29	1.48	0.4	0.55	0.81	2.67	0.68	0.58
11	61	0.1	0.8	0.8	0.8	Yes	Yes	0	0	0	3.37	0.27	0.21	0.1	3.81	0	0.17	0.15	4.12	0.1	0.22	0.17	4.99
12	81	CF	CF	CF	FC	Yes	Yes	0	0.06	0.71	3.55	0.07	0	1.91	8.52	0.23	0.15	2.49	13.12	0.19	0.21	3.85	14.01
13	67	0.1	0.3	0.5	0.3	Yes	Yes	0	1.73	N/A	N/A	0.05	2.15	N/A	N/A	0.2	3.43	N/A	N/A	0.77	5.63	N/A	N/A
14	63	0.05	CF	CF	CF	No	Yes	0.27	0.52	N/A	N/A	0.69	1.04	N/A	N/A	0.71	1.27	N/A	N/A	0.93	1.48	N/A	N/A
15	82	0.2	0.7	0.7	0.7	Yes	Yes	0.1	0.11	0.15	1.45	0.1	0.4	0.33	3.05	0.17	1.61	0.45	4.13	1.51	3.98	2.66	5.63
16	79	0.2	0.3	0.3	0.1	Yes	Yes	0	0	0.25	12.03	0	0	0.9	12.02	0	0	1.5	13.43	0	0	1.72	13.45
17	74	0.1	0.1	0.1	0.1	Yes	Yes	0	0	0	0	0.15	0.06	0.1	0.12	1	0.06	0.3	0.18	0.15	0.2	0.28	0.62
18	70	CF	0.5	0.2	0.2	Yes	Yes	0.1	0	0	0	0.27	0.15	0.38	0	0.35	0.55	0.4	0	0.35	0.62	0.48	0
19	55	0.3	1.0	1.0	1.0	Yes	Yes	0	0	1.07	0.65	0	0	2.17	4.25	0.82	0.68	3.26	7.84	0.89	0.25	3.43	8.28

Preop, preoperative; N/A, not applicable; FU, follow-up; dec, decimal; HM, hand motion; CF, counting fingers.

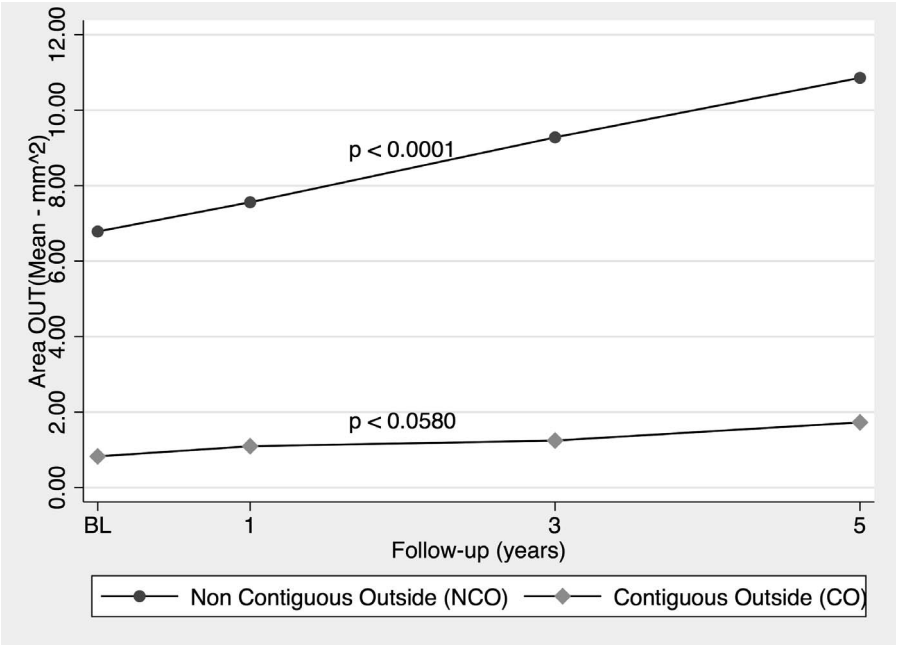

Figure 4. Mean change in GA extension in the CO and NCO zones at the different time points. Trend analysis revealed that atrophy progression was statistically significant among the NCO areas ($P < 0.0001$) but was not in the CO areas ($P < 0.058$). The P values represented here refer to the trend analysis.

The FAF patterns of the NCO and CO areas were assessed. The NCO group showed more severe FAF patterns compared with the CO group. The difference was statistically significant at every time point ($P < 0.0005$). The increased FAF developed rapidly after the surgery in the NCO areas and was already detectable at baseline in most of the cases (Figs. 3B, 3J, 3N). The CO areas did not show rapid FAF changes (Fig. 3F).

In addition, we observed a significant increase in the severity of FAF patterns next to the CNV in the eight eyes that developed this complication at the graft's edge. Figure 6 shows the difference in FAF patterns before and after the onset of marginal neovascularization in three representative cases.

There was a high agreement rate between the two observers: the Cohen kappa coefficient was between 0.57 and 0.97 and was statistically significant for each parameter ($P < 0.0001$).

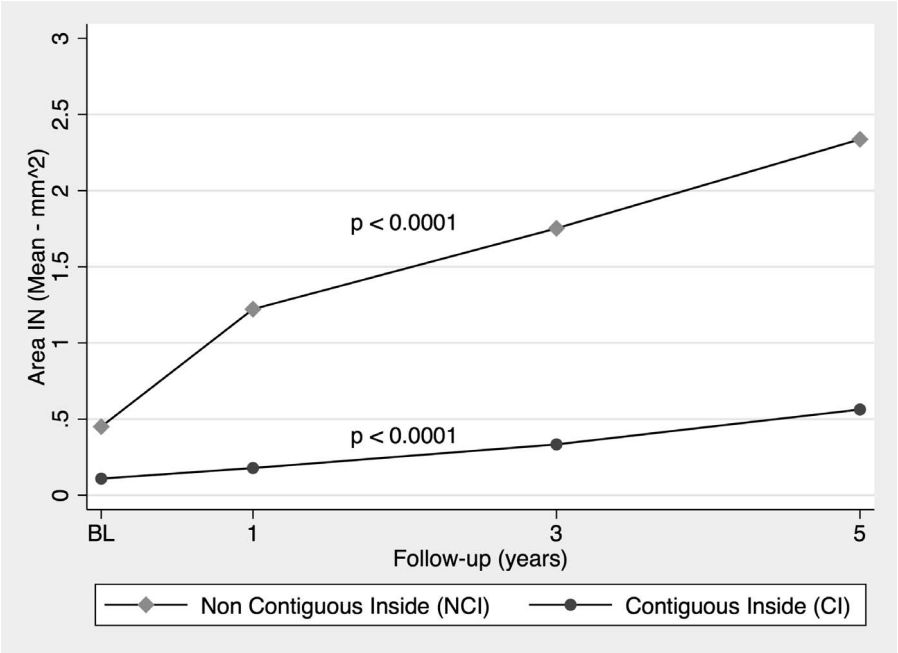

Figure 5. Mean change in GA in the CI and NCI zones at the different time points. Trend analysis revealed a statistically significant progression in both groups ($P < 0.0001$). Nevertheless, the NCI group exhibits a more rapid progression compare with the CI group. The P values represented here refer to the trend analysis.

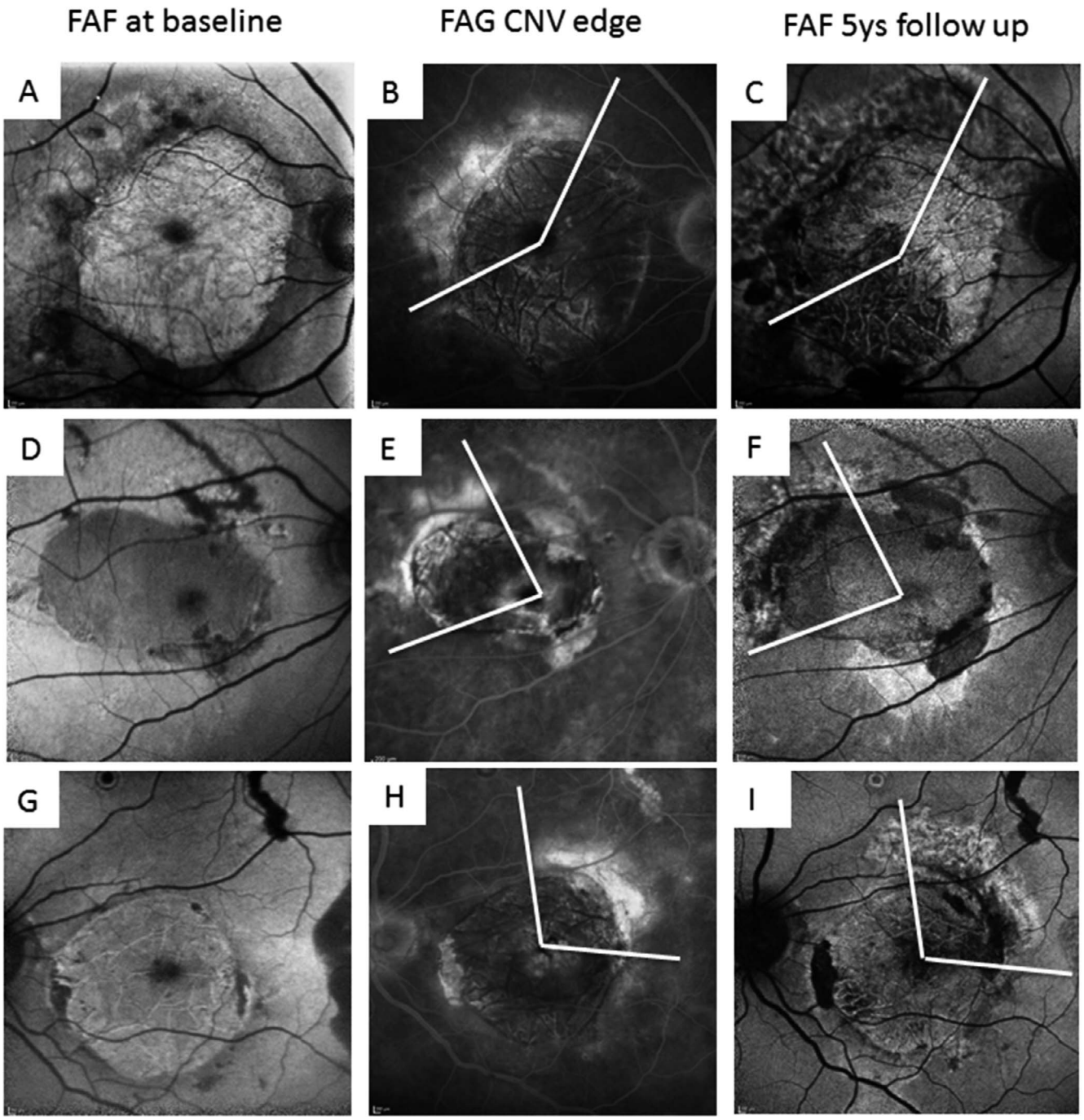

FIGURE 6. Representative examples of FAF changes in three eyes that developed CNV at the edge of the graft. The extension of CNV was evaluated on FAG and demarcated with *white lines* (**B**, **E**, **H**). The corresponding sectors developed a high-grade FAF pattern and atrophic changes during follow-up (**C**, **F**, **I**) compared with the baseline FAF (**A**, **D**, **G**).

DISCUSSION

RPE contiguity between the graft and the area of the posterior pole in which it is positioned seems to be a protective factor against atrophy progression. At the same time, a healthy RPE monolayer in contact with an area of atrophy appears to react to a stimulus that promotes its degeneration.

The progression of atrophy external to the graft is statistically significant in the NCO areas but it is not in the CO areas. Figure 3 shows the evolution of atrophy in four cases during the five years of follow-up. The difference between the first case, with no point of contact between native and transplanted RPE (Figs. 3A–D), and the second one, with nearly complete RPE contiguity (Figs. 3E–H), is impressive. The first case shows atrophy progression that involves both the native RPE in the posterior pole and the graft's RPE, whereas in the second case there is almost perfect preservation of the RPE after five years, except for a small area at the edge of the graft that was originally damaged during surgical manipulation. In the third (Fig. 3I–L) and fourth cases (Figs. 3M–P), the CO areas (full arrows) show minimal signs of atrophy after five years, whereas the NCO areas present significant atrophy progression both on the graft and the original RPE side (empty arrows). In

Investigative Ophthalmology & Visual Science

the cases reported in Figure 3, it can be observed that the distance from the fovea does not seem to influence the atrophy progression rate.

Other studies have shown that the area of atrophy surrounding the choroidal graft tends to enlarge over time,[18] and the graft's RPE may become atrophic in a short period of time, with a consequent loss of function.[19] Caramoy et al.[20] suggested that large choroidal grafts are more likely to retain a good functional outcome but could not explain the reason why. Most surgeons assumed that the main goal was to replace the CC-RPE complex underneath the macula and neglected the surrounding area. As there was no awareness that the RPE gap may influence the development of RPE atrophy, no special effort was generally made to extract a graft that could cover the entire naked RPE area.

We observed that the native RPE in the NCO areas tended to rapidly exhibit a high-grade FAF. There was a statistically significant difference in the FAF severity grade between NCO and the CO areas at all time points. Differently from GA, the RPE involved in the rapid FAF modification was not affected by drusen and displayed a normal FAF pattern before surgery (Fig. 3). The increased FAF was initially attributed to an accumulation of lipofuscin in a dysfunctional RPE unable to process it.[21] In particular, a lipofuscin compound, A2E, was proved to have significantly toxic effects on the RPE.[22,23] In this study, we observed that the RPE demonstrating considerable and rapid changes in FAF pattern was in contact with an area lacking a CC-RPE complex. A shortcoming in processing lipofuscin is unlikely to be the primary cause of the increased FAF, as an otherwise healthy RPE is involved in the process. The fact that the increased FAF pattern affects the NCO areas but not the CO areas, suggests that the changes in the FAF pattern are induced by modified homeostatic conditions resulting from a noncontiguous CC-RPE complex.

The CC-RPE gap may influence the surrounding tissues in different ways. Bruch's membrane acts as a sieve between the retina and the choroid[6]; therefore, its interruption may have an impact on the homeostasis of the subretinal space. The higher oxygen tension in the choroid,[24,25] in the absence of Bruch's membrane, may spread out to the RPE and the retina, causing damage from oxidative stress. In addition, the CC that has fenestrated endothelial cells,[26] again in the absence of Bruch's membrane, may allow the passage of proteins potentially toxic to the RPE. The transmission of toxic compounds from diseased to healthy cells is another possible mechanism that has been already recognized in other neurodegenerative diseases.[27]

Mones et al.[28] recently hypothesized that RPE cell activation and death via pyroptosis and necroptosis, secondary to the release of intracellular contents in areas of RPE discontinuities above drusen, may be responsible for GA development and progression. A vicious cell-to-cell cycle that further activates neighboring RPE cells and leads to an uncontrolled release of toxic intracellular material may promote GA expansion. A similar cascade of events, originating from the noncontiguous native-RPE/transplanted-RPE areas in our series, may result in RPE cell activation (high FAF pattern) and subsequent atrophy progression.

In the GAIN study,[29] the authors reported a correlation between FAF pattern and atrophy extension at baseline. Moreover, they found that the baseline area of atrophy was associated with GA growth independently of FAF patterns, concluding that the FAF patterns seemed to be a consequence of enlarging atrophy rather than the cause. The results of their study are consistent with our findings. The mean area of atrophy at baseline is significantly larger in the NCO group and tends to enlarge over time, more so than in the CO zone (Fig. 4). Biarnes et al.[29] suggested that the perimeter of the lesion may be correlated with the severity of the FAF pattern, as the longer the perimeter, the higher the number of atrophic RPE cells in direct contact with healthy cells. Our study does not support this theory, as the RPE defect at baseline is induced by surgical RPE removal and not by RPE degeneration. It is better assumed that the CC-RPE area gap triggers a cascade of events that eventually affect the originally healthy RPE, rather than sick RPE cells causing the degeneration of healthy ones.

The analysis of atrophy progression inside the graft shows a statistically significant increase in atrophy over time in both the CI and NCI groups (Fig. 5). Nevertheless, the enlargement of atrophy is more evident in the NCI zones. These data suggest that a gap of CC-RPE complex close to the graft provides a stimulus that promotes the development of atrophic changes, even on the graft side. Despite the atrophy evolution inside the graft, as this process usually progresses from the edge of the graft toward the center, only three eyes developed subfoveal RPE atrophy with subsequent visual deterioration during the follow-up period.

The graft is harvested in the midperiphery, in an area that usually does not develop atrophy in dry AMD. Based on this observation, one could expect the RPE to retain its original properties and show a certain degree of resistance toward atrophic changes. Unfortunately, this is not the case. Local factors that arise from the presence of a CC-RPE gap can trigger significant atrophy progression, including on CC-RPE derived from the midperiphery. However, a complete overlap between grafted and native RPE supports the preservation of the integrity of the graft (Figs. 3E–H). Nevertheless, even small defects of the graft's RPE in a CI zone (e.g. Figs. 3F–H, short empty arrow) show a statistically significant enlargement over time (Fig. 5). In fact, in this study, evidence was found that any CC-RPE defect tends to enlarge over time with an abrupt transition between the area of healthy RPE/photoreceptors and the area of chorioretinal atrophy.

We postulate that local factors can highly influence the development of atrophic changes in the same eye, as we observed areas of good RPE preservation next to areas of rapid atrophy progression. This represents a remarkable observation, as genetic and environmental features are expected to affect the eye homogeneously. It suggests that local homeostatic alterations can deeply affect RPE degeneration independently from genetic predisposition.

As an additional demonstration that the alteration of local conditions can promote RPE changes, we observed atrophy and high-grade FAF alterations of the RPE next to the CNV in eyes with this complication (Fig. 6). The process was self-limiting and did not involve the macula. Consequently, the visual function remained unaffected in all cases. We may speculate that this event is correlated with an increased concentration of VEGF at the border of the graft in the early postoperative period due to the reperfusion process inside the graft. This process resembles the progression of atrophic degeneration observed after anti-VEGF therapy.[3–5] Interestingly, we observed an increased FAF pattern and atrophic changes next to the CNV at the edge of the graft, despite its spontaneous fibrotic regression without any therapy. Further studies will be necessary to understand if the increased atrophy after anti-VEGF therapy is primarily due to the drug or whether it is secondary to local changes induced by the drug, such as fibrosis and RPE discontinuities correlated with CNV contraction.

An autologous full-thickness choroidal graft that reaches a rapid reperfusion[30] may represent the most biocompatible way to replace the sick CC-RPE complex in eyes with AMD. The RPE is already displaced in a monolayer on its physiologic substrate, Bruch's membrane, and there is no risk for immunoreactions. This model eliminates several variables

present in other studies that aimed to replace the RPE[31–37] and, from this perspective, it may provide interesting insights on the behavior of the healthy transplanted RPE and the surrounding native RPE. Based on this study and other observations,[28,38] one can assume that a gap in CC-RPE complex, which correlates to various pathologic circumstances, tends to enlarge over time. Therefore, the goal of the transplantation should be to cover the entire area of atrophic or missing RPE to minimize the risk of atrophy enlargement and transplanted RPE degeneration.

In conclusion, although this study describes the RPE changes after an autologous choroidal graft in a small number of patients, it can shed some light on the mechanism involved in RPE survival and atrophy progression. Further investigations will be necessary to fully understand the mechanisms involved in the progression of GA.

Acknowledgments

Disclosure: **G. Pertile**, None; **M. Mete**, None; **A. Peroglio Deiro**, None; **M. Guerriero**, None; **M. Sartore**, None; **A. Alfano**, None; **A. Polito**, None

References

1. Resnikoff S, Pascolini D, Etya'ale D, et al. Global data on visual impairment in the year 2002. *Bull World Health Organ*. 2004; 82:844–851.
2. Group CR, DF, Martin Maguire MG, et al. Ranibizumab and bevacizumab for neovascular age-related macular degeneration. *N Engl J Med*. 2011;364:1897–1908.
3. Ying GS, Maguire MG, Daniel E, et al. Association of baseline characteristics and early vision response with 2-year vision outcomes in the Comparison of AMD Treatments Trials (CATT). *Ophthalmology*. 2015;122:2523–2531.e1.
4. Grunwald JE, Pistilli M, Daniel E, et al. Incidence and growth of geographic atrophy during 5 years of Comparison of Age-Related Macular Degeneration Treatments Trials. *Ophthalmology*. 2017;124:97–104.
5. Hata M, Yamashiro K, Oishi A, et al. Retinal pigment epithelial atrophy after anti-vascular endothelial growth factor injections for retinal angiomatous proliferation. *Retina*. 2017;37: 2069–2077.
6. Bhutto I, Lutty G. Understanding age-related macular degeneration (AMD): relationships between the photoreceptor/retinal pigment epithelium/Bruch's membrane/choriocapillaris complex. *Mol Aspects Med*. 2012;33:295–317.
7. McLeod DS, Grebe R, Bhutto I, Merges C, Baba T, Lutty GA. Relationship between RPE and choriocapillaris in age-related macular degeneration. *Invest Ophthalmol Vis Sci*. 2009;50: 4982–4991.
8. van Romunde SH, Polito A, Bertazzi L, Guerriero M, Pertile G. Long-term results of full macular translocation for choroidal neovascularization in age-related macular degeneration. *Ophthalmology*. 2015;122:1366–1374.
9. Chen FK, Patel PJ, Uppal GS, et al. A comparison of macular translocation with patch graft in neovascular age-related macular degeneration. *Invest Ophthalmol Vis Sci*. 2009;50: 1848–1855.
10. Yamada Y, Miyamura N, Suzuma K, Kitaoka T. Long-term follow-up of full macular translocation for choroidal neovascularization. *Am J Ophthalmol*. 2010;149:453–457.e1.
11. Caramoy A, Liakopoulos S, Menrath E, Kirchhof B. Autologous translocation of choroid and retinal pigment epithelium in geographic atrophy: long-term functional and anatomical outcome. *Br J Ophthalmol*. 2010;94:1040–1044.
12. Eckardt C, Eckardt U. Macular translocation in nonexudative age-related macular degeneration. *Retina*. 2002;22:786–794.
13. Khurana RN, Fujii GY, Walsh AC, Humayun MS, de Juan E Jr, Sadda SR. Rapid recurrence of geographic atrophy after full macular translocation for nonexudative age-related macular degeneration. *Ophthalmology*. 2005;112:1586–1591.
14. Cahill MT, Mruthyunjaya P, Bowes Rickman C, Toth CA. Recurrence of retinal pigment epithelial changes after macular translocation with 360 degrees peripheral retinectomy for geographic atrophy. *Arch Ophthalmol*. 2005;123: 935–938.
15. van Romunde SHM, Polito A, Peroglio Deiro A, Guerriero M, Pertile G. Retinal pigment epithelium-choroid graft with a peripheral retinotomy for exudative age-related macular degeneration: long-term outcome [published online ahead of print November 16, 2017]. *Retina*. doi:10.1097/IAE.0000000000001945.
16. Cereda MG, Parolini B, Bellesini E, Pertile G. Surgery for CNV and autologous choroidal RPE patch transplantation: exposing the submacular space. *Graefes Arch Clin Exp Ophthalmol*. 2010;248:37–47.
17. Schmitz-Valckenberg S, Sahel JA, Danis R, et al. Natural history of geographic atrophy progression secondary to age-related macular degeneration (Geographic Atrophy Progression Study). *Ophthalmology*. 2016;123:361–368.
18. Chen FK, Uppal GS, MacLaren RE, et al. Long-term visual and microperimetry outcomes following autologous retinal pigment epithelium choroid graft for neovascular age-related macular degeneration. *Clin Exp Ophthalmol*. 2009;37:275–285.
19. MacLaren RE, Uppal GS, Balaggan KS, et al. Autologous transplantation of the retinal pigment epithelium and choroid in the treatment of neovascular age-related macular degeneration. *Ophthalmology*. 2007;114:561–570.
20. Caramoy A, Fauser S, Kirchhof B. Retinal stimuli can be restored after autologous transplant of retinal pigment epithelium and choroid in pigment epithelium tears. *Acta Ophthalmol*. 2011;89:e490–e495.
21. Schmitz-Valckenberg S, Fleckenstein M, Scholl HP, Holz FG. Fundus autofluorescence and progression of age-related macular degeneration. *Surv Ophthalmol*. 2009;54:96–117.
22. Sparrow JR, Zhou J, Cai B. DNA is a target of the photodynamic effects elicited in A2E-laden RPE by blue-light illumination. *Invest Ophthalmol Vis Sci*. 2003;44:2245–2251.
23. Zhou J, Jang YP, Kim SR, Sparrow JR. Complement activation by photooxidation products of A2E, a lipofuscin constituent of the retinal pigment epithelium. *Proc Natl Acad Sci U S A*. 2006;103:16182–16187.
24. Pournaras CJ, Riva CE, Tsacopoulos M, Strommer K. Diffusion of O2 in the retina of anesthetized miniature pigs in normoxia and hyperoxia. *Exp Eye Res*. 1989;49:347–360.
25. Alm A, Bill A. Blood flow and oxygen extraction in the cat uvea at normal and high intraocular pressures. *Acta Physiol Scand*. 1970;80:19–28.
26. Spitznas M, Reale E. Fracture faces of fenestrations and junctions of endothelial cells in human choroidal vessels. *Invest Ophthalmol*. 1975;14:98–107.
27. Guo JL, Lee VM. Cell-to-cell transmission of pathogenic proteins in neurodegenerative diseases. *Nat Med*. 2014;20: 130–138.
28. Monés J, Garcia M, Biarnés M, Lakkaraju A, Ferraro L. Drusen Ooze: A novel hypothesis in geographic atrophy. *Ophthalmology Retina*. 2017;1:461–473.
29. Biarnes M, Arias L, Alonso J, et al. Increased fundus autofluorescence and progression of geographic atrophy secondary to age-related macular degeneration: the GAIN Study. *Am J Ophthalmol*. 2015;160:345–353.e5.
30. van Zeeburg EJ, Cereda MG, van der Schoot J, Pertile G, van Meurs JC. Early perfusion of a free RPE-choroid graft in patients with exudative macular degeneration can be imaged

with spectral domain-OCT. *Invest Ophthalmol Vis Sci*. 2011; 52:5881–5886.

31. Binder S, Stanzel BV, Krebs I, Glittenberg C. Transplantation of the RPE in AMD. *Prog Retin Eye Res*. 2007;26:516–554.
32. da Cruz L, Chen FK, Ahmado A, Greenwood J, Coffey P. RPE transplantation and its role in retinal disease. *Prog Retin Eye Res*. 2007;26:598–635.
33. Nommiste B, Fynes K, Tovell VE, Ramsden C, da Cruz L, Coffey P. Stem cell-derived retinal pigment epithelium transplantation for treatment of retinal disease. *Prog Brain Res*. 2017;231:225–244.
34. Schwartz SD, Regillo CD, Lam BL, et al. Human embryonic stem cell-derived retinal pigment epithelium in patients with age-related macular degeneration and Stargardt's macular dystrophy: follow-up of two open-label phase 1/2 studies. *Lancet*. 2015;385:509–516.
35. Shirai H, Mandai M, Matsushita K, et al. Transplantation of human embryonic stem cell-derived retinal tissue in two primate models of retinal degeneration. *Proc Natl Acad Sci U S A*. 2016;113:E81–E90.
36. Stanzel BV, Liu Z, Somboonthanakij S, et al. Human RPE stem cells grown into polarized RPE monolayers on a polyester matrix are maintained after grafting into rabbit subretinal space. *Stem Cell Reports*. 2014;2:64–77.
37. Mandai M, Watanabe A, Kurimoto Y, et al. Autologous induced stem-cell-derived retinal cells for macular degeneration. *N Engl J Med*. 2017;376:1038–1046.
38. Curcio CA, Saunders PL, Younger PW, Malek G. Peripapillary chorioretinal atrophy: Bruch's membrane changes and photoreceptor loss. *Ophthalmology*. 2000;107:334–343.

Investigative Ophthalmology & Visual Science